phys. stat. sol. (b) **222**, 523 (2000)

Subject classification: 75.10.Jm; 78.47.+p; 78.66.Fd; S7.12

Dyakonov-Perel Effect on Spin Dephasing in n-Type GaAs

M.W. WU[1]) (a) and C.Z. NING (b)

(a) Chemistry Department, University of California, Santa Barbara, California 93106, USA

(b) Computational Quantum Optoelectronics, NASA Ames Research Center, M/S N229-1, Moffett Field, California 94035, USA

(Received April 25, 2000; in revised form June 23, 2000)

We study the spin dephasing in n-doped bulk GaAs under moderate magnetic fields in Voigt configuration due to the Dyakonov-Perel (DP) effect by constructing and numerically solving the kinetic Bloch equations. Both acoustic (AC) and longitudinal optical (LO) phonon scattering, together with impurity scattering, are included in our theory, and their contributions to the spin dephasing time under the DP effect are examined in detail. The spin dephasing time is obtained from the time evolution of the incoherently summed spin coherence. We investigate how the spin dephasing time is affected by temperature, impurity level, magnetic field, and electron density. In particular, our theory shows that spin dephasing time increases with increasing magnetic field. We find that, contrary to the prediction of previous simplified treatments of the DP effect, the spin dephasing time increases with temperature in the presence of impurity scattering. These results are in qualitative agreement with recent experiments.

1. Introduction

With the recent development of ultrafast nonlinear optical experiments [1–12], electron spin within semiconductors has become a focus of interest as it shows great potential to be used to store quantum coherence. For this purpose, the spin lifetime must be long enough to allow the processing of the stored information. For n-doped bulk GaAs, it is found experimentally that the spin lifetime can last up to 100 ns [10]. This finding has stimulated optimism that coherent electrons will finally be realized as a basis for quantum computation.

The electron spin coherence can be observed directly by femtosecond time-resolved Faraday rotation in the Voigt configuration. In that configuration a moderate magnetic field is applied normal to the growth axis of the sample. The coherence is introduced by a circularly polarized pump pulse that creates electrons and holes with an initial spin orientation normal to the magnetic field. Then the magnetic field causes the electron spin to flip back and forth along the growth axis which makes the net spin precess about the magnetic field. After a certain delay time τ, a linearly polarized probe pulse is sent into the sample along a direction slightly different from the pump pulse. By measuring the Faraday rotation angle, one can sensitively detect the net spin of electrons associated with the delay time τ. This method has proven to be extremely successful in measuring coherent spin evolution and spin dephasing [1, 2, 8–10].

[1]) Corresponding author; e-mail: mwu@chem.ucsb.edu

In order to explore spin-related device applications, it is important to understand the spin dephasing mechanism. Three such mechanisms have been proposed in semiconductors [13, 14]: the Elliott-Yafet (EY) mechanism [15, 16], the Dyakonov-Perel (DP) mechanism [17], and the Bir-Aronov-Pikus (BAP) mechanism [18]. In the EY mechanism, spin–orbit interaction leads to mixing of wave functions of opposite spins. This results in nonzero electron spin flip due to impurity and phonon scattering. The DP mechanism [17] is due to spin–orbit interaction in crystals without inversion center which results in spin state splitting of the conduction band at $k \neq 0$. This is equivalent to an effective magnetic field acting on the spin, with its magnitude and orientation depending on $\mathbf{k}$. Finally, the BAP mechanism [18] originates from mixing of heavy hole (hh) and light hole (lh) bands induced by spin–orbit coupling.[2]) Spin-flip scattering of electrons by holes due to Coulomb interaction is therefore permitted, which gives rise to spin dephasing.

For GaAs, the EY mechanism is less effective under most conditions, due to the large band gap and low scattering rate for high quality samples. The BAP mechanism is important for either p-doped or insulating GaAs. For n-doped samples, however, as holes are rapidly recombined with electrons due to the presence of a large number of electrons, spin dephasing due to the regular BAP mechanism is blocked. Therefore, the DP mechanism (or possibly the EY mechanism under certain conditions) is the main mechanism for spin dephasing.

Recently, we presented a kinetic theory to describe the spin precession in an undoped insulating $ZnSe/Zn_{1-x}Cd_xSe$ quantum well under moderate magnetic fields in the Voigt configuration [19]. With optical and spin coherence being clarified, we constructed the kinetic Bloch equations and calculated dephasing and relaxation kinetics of laser-pulse excited plasma due to statically screened Coulomb scattering and the electron–hole spin exchange effect (the BAP mechanism). (We also proposed in [19] another spin dephasing mechanism due to relativistic expansion of electron–hole Coulomb scattering. However, our recent first-principle calculation of the matrix element shows that this mechanism can be neglected for ZnSe and the scattering matrix element of electron–hole spin exchange in [19] should be considered only from the BAP mechanism.)

In this paper, we extend our theory to the case of n-doped bulk GaAs. For the reason stated above, we will focus on the DP mechanism and study how it affects spin dephasing. Moreover, we will study how moderate magnetic fields can change the spin lifetime. It was discovered experimentally that for highly n-doped samples the spin lifetime increases with increasing magnetic field, whereas for undoped or lightly doped samples the spin lifetime decreases with increasing magnetic field [10]. To our knowledge, this experimental result has not been discussed theoretically. For low and moderate magnetic fields, Landau splitting is unimportant and the magnetic field should not affect the spin dephasing time induced by the EY and/or BAP mechanisms. Therefore, the DP mechanism, alone or together with the other two mechanisms, should be responsible for the magnetic field dependence of the spin dephasing time.

Our theory is based on a two-spin-band model in the conduction band. As the spin dephasing time for n-doped samples is orders of magnitude longer than the optical dephasing time (of the order of a few hundred fs), and the pump pulse in the experi-

[2]) For bulk GaAs, the mixing happens not only at $k \neq 0$ points, but also strongly at the Γ point due to the degeneracy of hh and lh at that point. However, for the 2D case, the degeneracy at the Γ point is lifted and the mixing mainly happens at non-Γ points.

ments [8–10] is ultrashort (100 fs), the initial pump and optical dephasing process will not be considered. This means that we will not address questions such as how a circularly polarized pump pulse introduces optical coherence together with unbalanced electron distributions in spin-up and -down bands, and how the optical coherence dephases due to carrier–carrier scattering. Instead, we assume that at $t = 0$ all optical coherence together with the optically generated electron–hole pairs has vanished, and what remains of the initial pump pulse in the system is the unbalanced electron Fermi distributions in spin-up and -down conduction bands. The contribution of DP terms is turned on at $t = 0$. A kinetic theory with all the initial processes included has been given in our recent paper [19].

2. Model and Kinetic Equations

In the presence of a magnetic field $\mathbf{B}$ and with the DP effect included, the Hamiltonian of an electron in the conduction band $\varepsilon_{\mathbf{k}} = k^2/2m^*$ has the form

$$H = \sum_{\mathbf{k}\sigma\sigma'} \left\{ \varepsilon_{\mathbf{k}} + [g\mu_B \mathbf{B} + \mathbf{h}(\mathbf{k})] \cdot \frac{\boldsymbol{\sigma}_{\sigma\sigma'}}{2} \right\} c^{\dagger}_{\mathbf{k}\sigma} c_{\mathbf{k}\sigma'} + H_{\mathrm{I}} \,. \tag{1}$$

Here $\boldsymbol{\sigma}$ are the Pauli matrices. For bulk material, $\mathbf{h}(\mathbf{k})$, which is sometimes referred to as the Dresselhaus term [20], can be written as

$$h_x(\mathbf{k}) = \gamma k_x (k_y^2 - k_z^2) \,, \qquad h_y(\mathbf{k}) = \gamma k_y (k_z^2 - k_x^2) \,, \qquad h_z(\mathbf{k}) = \gamma k_z (k_x^2 - k_y^2) \,, \tag{2}$$

with $\gamma = (4/3)\,(m^*/m_{\mathrm{cv}})\,(1/\sqrt{2m^{*3}E_{\mathrm{g}}})\,(\eta/\sqrt{1-\eta/3})$ and $\eta = \Delta/(E_{\mathrm{g}} + \Delta)$. Here E_{g} denotes the band gap, Δ represents the spin–orbit splitting of the valence band, and m_{cv} is a constant close in magnitude to the free electron mass m_0 [14]. The interaction Hamiltonian H_{I} is composed of Coulomb interaction H_{ee}, electron–LO phonon interaction H_{LO}, electron–AC phonon interaction H_{AC}, as well as electron–impurity scattering H_{i}. Their expressions can be found in books [21, 22].

We construct the kinetic Bloch equations by the nonequilibrium Green function method [21] as follows:

$$\dot{\rho}_{\mathbf{k},\sigma\sigma'} = \dot{\rho}_{\mathbf{k},\sigma\sigma'}|_{\mathrm{coh}} + \dot{\rho}_{\mathbf{k},\sigma\sigma'}|_{\mathrm{scatt}} \,. \tag{3}$$

Here $\rho_{\mathbf{k},\sigma\sigma'}$ represents a single particle density matrix of the conduction bands. The diagonal elements describe the carrier distribution functions $\rho_{\mathbf{k},\sigma\sigma} = f_{\mathbf{k}\sigma}$ of wave vector $\mathbf{k}$ and spin σ. The off-diagonal elements $\rho_{\mathbf{k},\frac{1}{2}-\frac{1}{2}} \equiv \varrho_{\mathbf{k}}$ describe the inter-spin-band polarization components (coherences) for the spin coherence [19]. Note that $\rho_{\mathbf{k},-\frac{1}{2}\frac{1}{2}} = \rho^*_{\mathbf{k},\frac{1}{2}-\frac{1}{2}} = \varrho^*_{\mathbf{k}}$. Therefore, $f_{\mathbf{k}\frac{1}{2}}$, $f_{\mathbf{k}-\frac{1}{2}}$, and $\varrho_{\mathbf{k}}$ are the quantities to be determined from the Bloch equations.

The coherent part of the equation of motion for the electron distribution function is given by

$$\left.\frac{\partial}{\partial t} f_{\mathbf{k}\sigma}\right|_{\mathrm{coh}} = -2\sigma\{[g\mu_B B + h_x(\mathbf{k})]\,\mathrm{Im}\,\varrho_{\mathbf{k}} + h_y(\mathbf{k})\,\mathrm{Re}\,\varrho_{\mathbf{k}}\} + 4\sigma\,\mathrm{Im}\sum_{\mathbf{q}} V_{\mathbf{q}} \varrho^*_{\mathbf{k}+\mathbf{q}} \varrho_{\mathbf{k}} \,, \tag{4}$$

where $V_{\mathbf{q}} = 4\pi e^2/[\epsilon_0(q^2 + \kappa^2)]$ is the Coulomb matrix element under static screening with $\kappa^2 = 6\pi e^2 N_{\mathrm{e}}/(\epsilon_0 E_{\mathrm{F}})$. N_{e} denotes the total electron density, E_{F} stands for the Fermi

energy, and ϵ_0 is the static dielectric constant. In this paper, the magnetic field is assumed to be in the x-direction. The first term on the right hand side (RHS) of Eq. (4) describes spin precession of electrons under the magnetic field B as well as the effective magnetic field $\mathbf{h}$ due to the DP effect. The second term comes from the Fock term of the Coulomb interaction. The scattering terms of electron distributions in the Markovian limit are given by

$$\begin{aligned}\left.\frac{\partial f_{\mathbf{k}\sigma}}{\partial t}\right|_{\text{scatt}} = \Big\{ & -4\pi \sum_{\mathbf{q}\lambda} g^2_{\mathbf{q}\lambda}\, \delta(\varepsilon_{\mathbf{k}} - \varepsilon_{\mathbf{k}-\mathbf{q}} - \Omega_{\mathbf{q}\lambda})\, [N_{\mathbf{q}\lambda}(f_{\mathbf{k}\sigma} - f_{\mathbf{k}-\mathbf{q}\sigma}) \\ & + f_{\mathbf{k}\sigma}(1 - f_{\mathbf{k}-\mathbf{q}\sigma}) - \text{Re}\,(\varrho_{\mathbf{k}}\varrho^*_{\mathbf{k}-\mathbf{q}})] \\ & - 4\pi N_{\text{i}} \sum_{\mathbf{q}} U^2_{\mathbf{q}}\, \delta(\varepsilon_{\mathbf{k}} - \varepsilon_{\mathbf{k}-\mathbf{q}})\, [f_{\mathbf{k}\sigma}(1 - f_{\mathbf{k}-\mathbf{q}\sigma}) - \text{Re}\,(\varrho_{\mathbf{k}}\varrho^*_{\mathbf{k}-\mathbf{q}})]\Big\} \\ & - \{\mathbf{k} \leftrightarrow \mathbf{k} - \mathbf{q}\}\ , \end{aligned} \tag{5}$$

in which $\{\mathbf{k} \leftrightarrow \mathbf{k} - \mathbf{q}\}$ stands for the same terms as in the previous $\{\ \}$ but with the interchange $\mathbf{k} \leftrightarrow \mathbf{k} - \mathbf{q}$. The first term inside the braces on the RHS of Eq. (5) comes from the electron–phonon interaction. λ stands for different phonon modes, i.e., one LO mode, one longitudinal AC mode due to the deformation potential, and two AC modes due to the transverse piezoelectric field. $g_{\mathbf{q}\lambda}$ are the matrix elements of electron–phonon coupling for mode λ. For LO phonons, $g^2_{\mathbf{q}\text{LO}} = 4\pi\alpha\Omega^{3/2}_{\text{LO}}/(\sqrt{2\mu}q^2)$ with $\alpha = e^2\sqrt{\mu/(2\Omega_{\text{LO}})}\,(\epsilon^{-1}_{\infty} - \epsilon^{-1}_0)$. ϵ_∞ is the optical dielectric constant and Ω_{LO} is the LO phonon frequency. For longitudinal phonons due to a deformation potential, $g^2_{\mathbf{q},\text{l}} = \Xi^2 q/2dv_{\text{sl}}$ with Ξ being the acoustic deformation potential, d the GaAs volume density, and v_{sl} representing longitudinal sound velocity. The corresponding phonon frequency is $\Omega_{\mathbf{q}\text{l}} = v_{\text{sl}}q$. There are two transverse AC phonon modes due to the piezoelectric field, and their contribution to electron–phonon coupling elements is given by $\sum_{j=1,2} g^2_{\mathbf{q}\text{t}_j} = 32\pi^2e^2e^2_{14}[q^2_xq^2_y + q^2_yq^2_z + q^2_zq^2_x - (3q_xq_yq_z)^2/q^2]/(\epsilon^2_0 dv_{\text{st}}q^5)$, with e_{14} being the piezoelectric constant and v_{st} denoting the transverse sound velocity. The corresponding phonon frequency is $\Omega_{\mathbf{q}\text{t}} = v_{\text{st}}q$. The second term inside the braces on the RHS of Eq. (5) results from electron–impurity scattering under random phase approximation with N_{i} denoting the impurity density. $U_{\mathbf{q}} = 4\pi Z_{\text{i}}e^2/[\epsilon_0(q^2 + \kappa^2)]$ and Z_{i} is the charge number of the impurity. Z_{i} is assumed to be 1 throughout our calculation. $N_{\mathbf{q}\lambda} = 1/[\exp(\Omega_{\mathbf{q}\lambda}/k_{\text{B}}T) - 1]$ is the Bose distribution of phonon mode λ at temperature T. It is noted that here and hereafter the Coulomb interaction is kept only at the Hartree-Fock level. As we mentioned previously, we assumed that all fast optical processes due to Coulomb scattering have been completed. A Fermi distribution has been reached before we turn on the DP term $\mathbf{h}(\mathbf{k})$ (Eq.(2)) in each spin band. In general, it is also necessary to keep the Coulomb scattering to guarantee that the carrier system relaxes back to the Fermi distribution after being driven away from the original Fermi distribution by magnetic field induced spin flipping between the two spin bands. However, the maximum imbalance of the electrons in the spin-up and -down bands in the experiments is at least two orders of magnitude smaller than the total electron density. Therefore the non-equilibrium carrier distribution further introduced in each spin band by the magnetic field is marginal since the electron distribution in each spin band is always in quasi-equilibrium. Hence in the present case Coulomb scattering is of marginal importance and we only include electron–phonon and/or electron–impurity scattering in our calculation.

Similarly, the coherent and scattering parts of the spin coherence are given by

$$\left.\frac{\partial \varrho_{\mathbf{k}}}{\partial t}\right|_{\text{coh}} = -ih_z(\mathbf{k})\,\varrho_{\mathbf{k}} + \frac{1}{2}\,[ig\mu_B B + ih_x(\mathbf{k}) + h_y(\mathbf{k})]\,(f_{\mathbf{k}\frac{1}{2}} - f_{\mathbf{k}-\frac{1}{2}}) + i\sum_{\mathbf{q}} V_{\mathbf{q}}(f_{\mathbf{k}+\mathbf{q}\frac{1}{2}} - f_{\mathbf{k}+\mathbf{q}-\frac{1}{2}})\,\varrho_{\mathbf{k}} - i\sum_{\mathbf{q}} V_{\mathbf{q}}\varrho_{\mathbf{k}+\mathbf{q}}(f_{\mathbf{k}\frac{1}{2}} - f_{\mathbf{k}-\frac{1}{2}})\,, \tag{6}$$

$$\left.\frac{\partial \varrho_{\mathbf{k}}}{\partial t}\right|_{\text{scatt}} = \Big\{2\pi\sum_{\mathbf{q}} \lambda g^2_{\mathbf{q}\lambda}\,\delta(\varepsilon_{\mathbf{k}} - \varepsilon_{\mathbf{k}-\mathbf{q}} - \Omega_{\mathbf{q}\lambda})\,[\varrho_{\mathbf{k}-\mathbf{q}}(f_{\mathbf{k}\frac{1}{2}} + f_{\mathbf{k}-\frac{1}{2}}) + (f_{\mathbf{k}-\mathbf{q}\frac{1}{2}} + f_{\mathbf{k}-\mathbf{q}-\frac{1}{2}} - 2)\,\varrho_{\mathbf{k}} - 2N_{\mathbf{q}\lambda}(\varrho_{\mathbf{k}} - \varrho_{\mathbf{k}-\mathbf{q}})] + 2\pi N_{\text{i}}\sum_{\mathbf{q}} U^2_{\mathbf{q}}\,\delta(\varepsilon_{\mathbf{k}} - \varepsilon_{\mathbf{k}-\mathbf{q}})\,[(f_{\mathbf{k}\frac{1}{2}} + f_{\mathbf{k}-\frac{1}{2}})\,\varrho_{\mathbf{k}-\mathbf{q}} - (2 - f_{\mathbf{k}-\mathbf{q}\frac{1}{2}} - f_{\mathbf{k}-\mathbf{q}-\frac{1}{2}})\,\varrho_{\mathbf{k}}]\Big\} - \{\mathbf{k} \leftrightarrow \mathbf{k} - \mathbf{q}\}\,. \tag{7}$$

Notwithstanding the fact that we call Eqs. (4) and (6) the "coherent" parts of the equations of motion, the spin dephasing comes from the anisotropic property of the DP term $\mathbf{h}(\mathbf{k})$ in these parts. If one takes $\mathbf{h} = 0$, electron–phonon and electron–impurity scattering alone cannot introduce any spin dephasing. This can be seen from the fact that $\sum_{\mathbf{k}} \left.\frac{\partial \varrho_{\mathbf{k}}}{\partial t}\right|_{\text{scatt}} = 0$ [19].

The initial conditions at $t = 0$ are taken as

$$\varrho_{\mathbf{k}}|_{t=0} = 0\,, \tag{8}$$

$$f_{\mathbf{k}\sigma}|_{t=0} = 1/\{\exp\,[(\varepsilon_{\mathbf{k}} - \mu_\sigma)/k_{\text{B}}T] + 1\}\,, \tag{9}$$

where μ_σ is the chemical potential for spin σ. The condition $\mu_{\frac{1}{2}} \neq \mu_{-\frac{1}{2}}$ gives rise to the imbalance of the carrier densities of the two spin bands. Equations (3) through (7) together with the initial conditions Eqs. (8) and (9) comprise the complete set of kinetic Bloch equations of our investigation.

3. Numerical Results

Before we present our numerical results, we would like to emphasize the spirit of our approach. As one notices, all the unknowns to be solved appear in the scattering terms. Specifically, the electron distribution function is no longer a Fermi distribution because of the existence of the anisotropic DP term $\mathbf{h}(\mathbf{k})$. This term in the coherent part drives the electron distribution away from an isotropic Fermi distribution, and the scattering terms attempt to randomize electrons in $\mathbf{k}$-space. Obviously, both the coherent part and the scattering terms have to be solved self-consistently to obtain the distribution function and the spin coherence.

We numerically solve the kinetic Bloch equations in such a self-consistent fashion to study the spin precession between the spin-up and -down bands. While we include electron–phonon scattering for all cases, electron–impurity scattering is sometimes excluded. As discussed in our previous paper [19], irreversible [23] spin dephasing is well defined by the envelope of the incoherently summed spin coherence $\rho(t) = \sum_{\mathbf{k}} |\varrho_{\mathbf{k}}(t)|$. In the following we will therefore plot the time evolution of $\rho(t)$ and the electron density $N_\sigma = \sum_{\mathbf{k}} f_{\mathbf{k}\sigma}$ of spin σ. The material parameters of GaAs for our calculation are tabulated in Table 1 [24]. m_{cv} is taken to be 0.5 m_0 throughout the calculation. Due to the

Table 1
Parameters used in the numerical calculations

κ_∞	10.8	κ	12.9
Ω_{LO}	35.4 meV	Ξ	7 eV
m^*	$0.067m_0$	d	5.3×10^3 kg/m^3
v_{sl}	5.29×10^3 m/s	v_{st}	2.48×10^3 m/s
e_{14}	1.41×10^9 V/m	Δ	0.341 eV
g	0.44	E_g	1.55 eV

anisotropic property of the DP effect, we have to distinguish all six **k**-directions: $\pm k_i$ ($i = x$, y, and z). We truncate each k_i from $-K_{cut}$ to K_{cut} with $K_{cut} \equiv \sqrt{2m^*(3E_F)}$. Instead of dividing $[-K_{cut}, K_{cut}]$ equally in **k**-space, we divide the energy domain $[0, 3E_F]$ into M segments of equal size to facilitate the evaluation of energy conservation (δ-functions) in the scattering terms of Eqs. (5) and (7). The corresponding **k**-space grid points are $-\sqrt{(M-1)/M}\,K_{cut}$, $\cdots$, $-K_{cut}/\sqrt{M}$, 0, $K_{cut}/\sqrt{M}$, $\cdots$, $\sqrt{(M-1)/M}\,K_{cut}$, where we take values of $f_{\mathbf{k}\sigma}$ and $\varrho_{\mathbf{k}}$. The total number of summations of each scattering term in calculating the Bloch equations scales as $M_s = (2M-1)^6$. This prevents us from taking a large value for M. In our calculation $M = 7$ is assumed, which gives $M_s \approx 4.8 \times 10^6$. It is understood that the small sampling of **k**-space renders our results quantitatively less accurate. However, we have verified the accuracy by varying the number of **k**-points with M up to 11. The results reported here are qualitatively accurate. Our main results are plotted in Figs. 1 to 5.

In Figs. 1 to 4 the total electron density in the two spin bands is $N_e = 10^{23}$ m^{-3}, whereas the density in the spin-up band is about 5×10^{20} m^{-3} higher than in the spin-down band at $t = 0$. This imbalance is assumed to be initially introduced by a circularly polarized pump pulse.

In Fig. 1 we plot the electron density in the spin-up and -down bands together with the incoherently summed spin coherence as a function of time for $B = 1$ T, $T = 30$ K, and impurity density $N_i = 0$. It is seen from the figure that excess electrons in the spin-up band start to flip to the spin-down band at $t = 0$ due to the presence of the magnetic

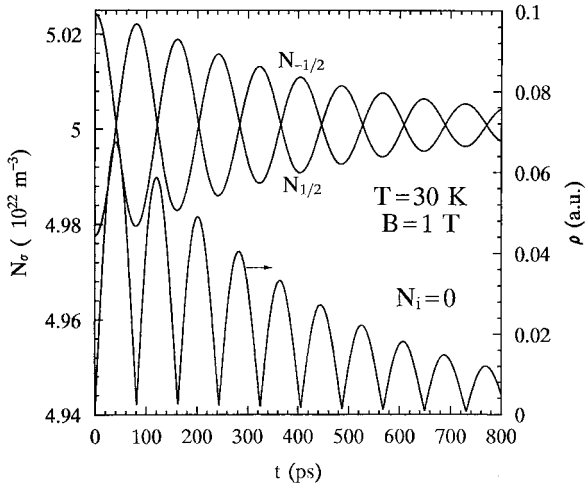

Fig. 1. Electron density N_σ in spin band σ and incoherently summed spin coherence ρ are plotted as a function of time t for $T = 30$ K and $B = 1$ T. Impurity scattering is not included. Note that the scale of the spin coherence is on the right side of the figure

field. In the meantime the spin coherence ρ accumulates. At about 40 ps, the electron densities in the two spin bands become equal and the spin coherence reaches the maximum. Then the spin coherence starts to feed back and the electron density in the spin-down band exceeds that in the spin-up band while ρ decreases. At about 79 ps, ρ reaches 0, whereas the density difference in the two spin bands reaches the maximum again with the excess electrons now in the spin-down band. Had there been no spin dephasing, the density of electrons in the spin-down band would have reached the same height as that in the spin-up band at $t = 0$. However, due to spin dephasing the second peak is lower than the first one. This oscillation goes on until the amplitude of the oscillation becomes zero due to spin dephasing. Differing from the case of an insulating semiconductor where holes play an important role and the beating frequency is determined by Zeeman splitting, redshifted by the Hartree-Fock type of Coulomb interaction and BAP scattering [19], the beating frequency here is mainly determined by Zeeman splitting. The contribution of the Hartree-Fock term in Eq. (6) is negligible in this n-doped case.

We plot the incoherently summed spin coherence as a function of time t for $T = 30$ K and $B = 1$ T in Figs. 2a and b with $N_i = 0$ and 0.01 N_e, respectively. The envelopes of $\rho(t)$ are also plotted in the same figures for $B = 1$, 2, 4, and 6 T. From the slope of the envelope function one obtains the spin dephasing times τ_s which are plotted versus

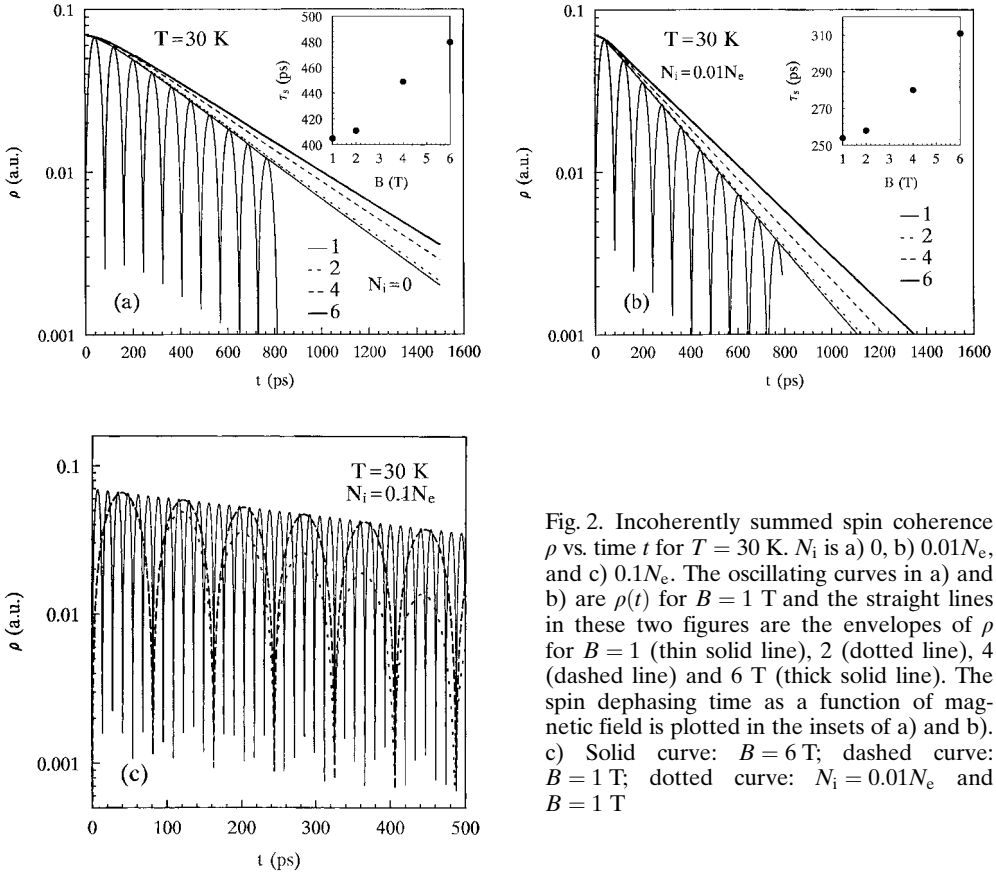

Fig. 2. Incoherently summed spin coherence ρ vs. time t for $T = 30$ K. N_i is a) 0, b) $0.01N_e$, and c) $0.1N_e$. The oscillating curves in a) and b) are $\rho(t)$ for $B = 1$ T and the straight lines in these two figures are the envelopes of ρ for $B = 1$ (thin solid line), 2 (dotted line), 4 (dashed line) and 6 T (thick solid line). The spin dephasing time as a function of magnetic field is plotted in the insets of a) and b). c) Solid curve: $B = 6$ T; dashed curve: $B = 1$ T; dotted curve: $N_i = 0.01N_e$ and $B = 1$ T

the magnetic field in the insets of the same figures. By comparing the insets of Figs. 2a and b, we note that the spin dephasing time decreases when impurities are introduced. However, if we further increase the impurity density from $N_i = 0.01\ N_e$ in Fig. 2b to $N_i = 0.1\ N_e$ in Fig. 2c, the spin dephasing time increases again. The slope of the solid ($B = 6$ T) and the dashed curve ($B = 1$ T) in Fig. 2c gives a dephasing time of about 714 ps, whereas the dotted curve for $B = 1$ T and $N_i = 0.01\ N_e$ in the same figure results in the dephasing time being 254 ps. In Fig. 2c, we also notice that the difference of spin dephasing time between different magnetic fields is negligible, as the dashed and the solid curve have almost the same slope.

This interesting property that spin dephasing time changes with impurity levels can be understood as follows. First, neither the DP term nor the scattering terms alone can introduce spin dephasing. They need to be combined to induce spin dephasing [17]. Therefore, when there is no scattering, spin lifetime is infinite. Introduction of scattering into such an anisotropic system reduces spin lifetime. This can be seen in Fig. 2a where electron–phonon scattering reduces spin lifetime. The same is true when we put impurities at $N_i = 0.01\ N_e$ into the system. However, scattering also redistributes electrons in momentum space and tends to lead them towards an isotropic distribution. As a result, when we further increase the impurity density by one order of magnitude, the anisotropy introduced by the DP effect is suppressed, and the spin dephasing time increases. Moreover, our results show that with the suppression of the DP effect, the magnetic field dependence of spin dephasing time is also suppressed, as we mentioned above.

We now consider the temperature dependence of the spin dephasing time. In Fig. 3, spin dephasing time τ_s is plotted against magnetic field for three typical temperatures $T = 5$, 30, and 100 K, where phonons play different roles in the scattering. At $T = 5$ K, the electron–phonon scattering does not make any contribution and electron–impurity scattering is the only scattering mechanism. Indeed, at this temperature we find no spin dephasing when we switch off impurity scattering by setting $N_i = 0$. Therefore spin dephasing at $T = 5$ K in Fig. 3 is purely due to impurity scattering. In addition to electron–impurity scattering, electron–AC phonon scattering starts to make a contribution at higher temperatures such as at $T = 30$ K. At a still higher temperature ($T = 100$ K), electron–LO phonon scattering becomes important. More importantly, our theory predicts that the spin lifetime increases as the temperature rises in the presence of impurities. This property is opposite to the results of earlier simplified treatments of the DP effect, where

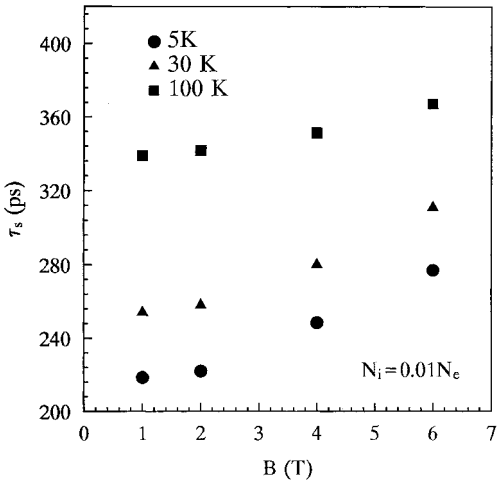

Fig. 3. Spin dephasing time τ_s as a function of magnetic field under three different temperatures $T = 5$, 30, and 100 K. $N_i = 0.01\ N_e$

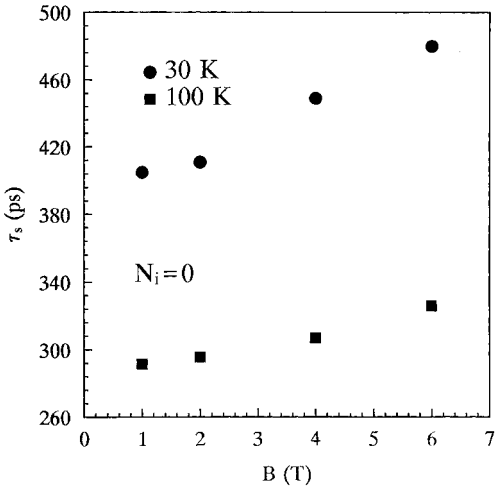

Fig. 4. Spin dephasing time τ_s as a function of magnetic field for temperature $T = 30$ and 100 K. $N_i = 0$

it was predicted that the spin lifetime decreases with increasing temperature in either bulk [17] or 2D systems [25]. However, a recent experiment by Ohno et al. [12] showed that the spin lifetime increases uniquely with increasing temperature for an n-doped GaAs quantum well. For n-type bulk GaAs, Kikkawa et al. [10] also showed that the spin lifetime increases with temperature up to 50 K in one case. The physics of this feature now seems clear: When temperature increases, electron–impurity scattering becomes stronger which, as discussed above, suppresses the anisotropy introduced by the DP effect. Therefore the spin lifetime is increased. However, at a higher impurity level (say, $N_i = 0.1\ N_e$), it is found from our calculation that the spin dephasing time is rather insensitive to the temperature, although it increases slightly with rising temperature.

It is interesting to note that with increasing temperature the electron–phonon scattering-induced momentum redistribution is much less efficient in destroying the anisotropy than that induced by electron–impurity scattering. Instead, in the impurity-free case, the DP dephasing mechanism increases more efficiently with temperature. As a result, the spin lifetime decreases significantly with increasing temperature, contrary to the case with impurities. This can be seen from Fig. 4, in which the spin dephasing time τ_s is plotted versus B for $T = 30$ K and 100 K. We did not include τ_s for the 5 K case as the spin lifetime is almost infinite at this temperature for the impurity-free case.

Let us now move on to the magnetic field dependence of the spin dephasing time. In the insets of Figs. 2a and b as well as in Figs. 3 and 4, a common feature is that the spin dephasing time increases with magnetic field. This feature persists at all impurity densities, temperatures, and electron densities (see Fig. 5 in the following) we have simulated. This is consistent with what was measured in an experiment by Kikkawa et al. for high electron density cases [10]. A plausible explanation is as follows: The magnetic field forces electrons to precess around it. This precession introduces additional symmetry in the momentum space which limits the **k**-space available to the DP effect which is anisotropic in it. Therefore the spin lifetime increases with magnetic field. Furthermore, we notice that the magnetic field dependence of the spin dephasing time is suppressed at higher impurity levels, as shown by Fig. 2c, or at higher temperatures, as shown in Fig. 3 (see the filled squares). This is because the new symmetry induced by the magnetic field has little effect once the system is already more or less randomized in **k**-space by the high impurity level.

Now we turn to the problem of density dependence of spin dephasing. In Fig. 5 we plot the spin dephasing time as a function of the magnetic field for an electron density $N_e = 10^{22}$ m^{-3}, which is one order of magnitude lower than in the previous case, and

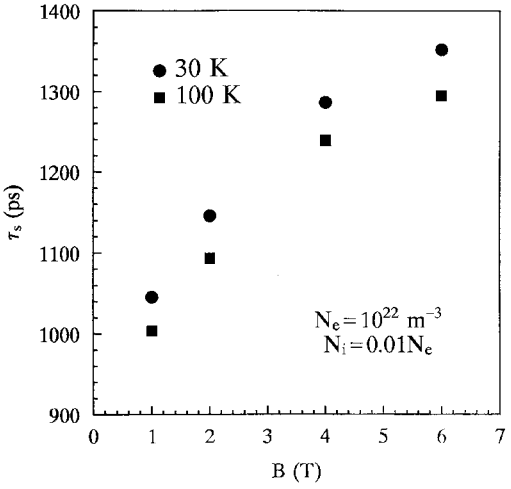

Fig. 5. Spin dephasing time τ_s as a function of magnetic field for temperature $T = 30$ and 100 K. $N_e = 10^{22}$ m^{-3} and $N_i = 0.01\ N_e$

temperatures $T = 30$ and 100 K. At $t = 0$, the electron density in the spin-up band is 2×10^{20} m^{-3} higher than that in the spin-down band. The impurity density is $N_i = 0.01\ N_e$. It can be seen from the figure that the spin lifetime now becomes much longer, rising from hundreds of picoseconds in the previous case to nanoseconds. This is because the DP effect (Eq. (2)) is proportional to k_F^3 and therefore proportional to N_e. When we decrease the electron density, the DP term becomes less important. Therefore, the spin lifetime becomes much longer. Similar to the former high density case, it is also noted in Fig. 5 that the spin lifetime increases with the magnetic field. This is not in agreement with what was seen in the experiment by Kikkawa et al. [10]. They reported that the spin lifetime decreases with increasing magnetic field at low electron density. The physics behind that experimental result is still unclear to us and more investigations are required.

4. Conclusion

In conclusion, we have performed a systematic investigation of the DP effect on the spin dephasing of n-type GaAs under moderate magnetic fields in Voigt configuration. Based on the nonequilibrium Green's function theory, we derived a set of kinetic Bloch equations for a two-spin-band model for the conduction band. This model includes electron–acoustic phonon, electron–LO phonon, and electron–impurity scattering. Electron–electron scattering is kept only to the Hartree-Fock level. By numerically solving the kinetic Bloch equations, we study the time evolution of electron densities in each spin band and the spin coherence – the correlation between spin-up and -down bands. The spin dephasing time is calculated from the slope of the envelope of the time evolution of the incoherently summed spin coherence. We therefore are able to study in detail how this dephasing time is affected by temperature, impurity level, magnetic field, and electron density. As the nature of the anisotropic system requires quite a large number of grid points in three dimensional **k**-space, even a modern high performance computer system is still restricted from taking a larger number of points to self-consistently solve the kinetic Bloch equations. Therefore, our results are only qualitatively accurate. Moreover, the parameter m_{cv} in the DP term is only known to be close in magnitude to the free electron mass [14]. In our calculation, this somewhat arbitrary number is assumed to be $0.5m_0$. (If we take $m_{cv} = m_0$ in our calculation, the spin dephasing time in Fig. 4 will be 1.22 ns when $B = 6$ T and $T = 100$ K.) In order to achieve a more accurate prediction of spin dephasing time, a first-principle calculation of this quantity is needed.

Nevertheless, we believe that the main results of this paper are valid. First, we find that the spin dephasing time depends sensitively on the impurity level. When we increase the impurity density from 0 to 0.01 N_e at a given temperature (therefore electron–phonon scattering is fixed), the spin dephasing time decreases. However, if we further increase the impurity density to 0.1 N_e, the spin dephasing time increases. This is explained by the dual role played by scattering, especially electron–impurity scattering. On the one hand, scattering induces spin dephasing through the anisotropic DP term. On the other hand, scattering also reduces the anisotropy through momentum space randomization which in turn increases the spin dephasing time. As a consequence, one observes that the spin dephasing time first decreases when the impurity is added. Above a critical impurity density, the spin dephasing time increases again. It is important to point out that, when the impurity density becomes too high, another spin dephasing mechanism, the EY mechanism [15, 16] which is not important for GaAs when the impurity density is not too high, may become important and will decrease the spin dephasing time. Therefore both mechanisms should be included if we want to maximize the spin coherence time at an optimal impurity density.

In the absence of impurity scattering, the spin dephasing time decreases when temperature rises. Nevertheless, in the presence of moderate impurities, our self-consistent kinetic calculation shows that spin dephasing time increases with increasing temperature. This is contrary to the result of earlier simplified calculations where the DP effect induced spin dephasing time always decreases with temperature [17, 25]. However, our result agrees with the findings of experiments [10, 12]. The physics of this feature is again due to the role played by electron–impurity scattering in bringing the system towards a more isotropic state. This becomes more efficient when temperature rises and therefore weakens the anisotropic property of the DP effect.

Our calculation also shows that due to the fact that the DP effect is proportional to the electron density, the spin dephasing time increases when the electron density decreases. This result is consistent with experimental findings [10]. Finally, our calculation shows that the spin dephasing time depends on the magnetic field. Our results indicate that the spin lifetime rises when the magnetic field increases. For the high electron density case, this is exactly what was found in the experiment by Kikkawa et al. [10]. However, for low density the experiment shows the opposite trend. The physics behind the low electron density case, together with the EY mechanism for the high impurity density case, is still under investigation and the results will be published in a separate paper.

Acknowledgements J. M. Kikkawa is acknowledged for providing information about his pertinent experimental work. M.W.W. also wishes to thank Dr. Yu. Takahashi for valuable discussion. We thank S. Cheung for his help in parallelizing our computer simulation code on a Silicon Graphics Origin Cluster. M.W.W. is supported by NASA Ames University Consortium NCC2-5368, and also partially by the National Science Foundation under Grant No. CHE 94-12410, CHE 97-09038 and CDA 96-01954, and by Silicon Graphics Inc.

Note added in proof After acceptance of this manuscript, we noticed the latest experiment by Kikkawa and Awschalom [26], which shows that the periodic pump pulse train in the experiments [8–10, 12] may cause nuclear spin polarization, and the polarized

nuclear spin can further cause the electron spin dephasing. The dephasing time induced by this mechanism should also increase with temperature as the nuclear spin polarization becomes weaker at a higher temperature. Therefore, more experiments are necessary for exploring the impurity effect proposed in our paper in order to get the optimal doping density and temperature for a maximum spin lifetime. This can be achieved, e. g., by sending radio frequency signals to remove the nuclear polarization and by varying the impurity level.

References

[1] T.C. Damen, L. Vina, J.E. Cunningham, J. Shah, and L.J. Sham, Phys. Rev. Lett. **67**, 3432 (1991).
[2] J. Wagner, H. Schneider, D. Richards, A. Fischer, and K. Ploog, Phys. Rev. B **47**, 4786 (1993).
[3] J.J. Baumberg, S.A. Crooker, D.D. Awschalom, N. Samarth, H. Luo, and J.K. Furdyna, Phys. Rev. Lett. **72**, 717 (1994); Phys. Rev. B **50**, 7689 (1994).
[4] A.P. Heberle, W.W. Rühle, and K. Ploog, Phys. Rev. Lett. **72**, 3887 (1994).
[5] C. Buss, R. Frey, C. Flytzanis, and J. Cibert, Solid State Commun. **94**, 543 (1995).
[6] S.A. Crooker, J.J. Baumberg, F. Flack, N. Samarth, and D.D. Awschalom, Phys. Rev. Lett. **77**, 2814 (1996); Phys. Rev. B **56**, 7574 (1997).
[7] C. Buss, R. Pankoke, P. Leisching, J. Cibert, R. Frey, and C. Flytzanis, Phys. Rev. Lett. **78**, 4123 (1997).
[8] J.M. Kikkawa, I.P. Smorchkova, N. Samarth, and D.D. Awschalom, Science **277**, 1284 (1997).
[9] J.M. Kikkawa and D.D. Awschalom, Nature **397**, 139 (1998).
[10] J.M. Kikkawa and D.D. Awschalom, Phys. Rev. Lett. **80**, 4313 (1998).
[11] H. Ohno, Science **281**, 951 (1998).
[12] Y. Ohno, R. Terauchi, T. Adachi, F. Matsukura, and H. Ohno, Phys. Rev. Lett. **83**, 4196 (1999).
[13] F. Meier and B.P. Zacharchenya (Eds.), Optical Orientation, North-Holland, Amsterdam 1984.
[14] A.G. Aronov, G.E. Pikus, and A.N. Titkov, Zh. Eksp. Teor. Fiz. **84**, 1170 (1983) [Sov. Phys. – JETP **57**, 680 (1983)].
[15] Y. Yafet, Phys. Rev. **85**, 478 (1952).
[16] R.J. Elliot, Phys. Rev. **96**, 266 (1954).
[17] M.I. Dyakonov and V.I. Perel, Zh. Eksp. Teor. Fiz. **60**, 1954 (1971) [Soviet Phys. – JETP **38**, 1053 (1971)].
[18] G.L. Bir, A.G. Aronov, and G.E. Pikus, Zh. Eksp. Teor. Fiz. **69**, 1382 (1975) [Soviet Phys. – JETP **42**, 705 (1975)].
[19] M.W. Wu and H. Metiu, Phys. Rev. B **61**, 2945 (2000).
[20] G. Dresselhaus, Phys. Rev. **100**, 580 (1955).
[21] H. Haug and A.P. Jauho, Quantum Kinetics in Transport and Optics of Semiconductors, Springer-Verlag, Berlin 1996.
[22] G.D. Mahan, Many-Particle Physics, Plenum, New York 1981.
[23] T. Kuhn and F. Rossi, Phys. Rev. Lett. **69**, 977 (1992).
[24] O. Madelung, M. Schultz, and H. Weiss (Eds.), Numerical Data and Functional Relationships in Science and Technology, Landolt-Börnstein, New Series, Vol. 17, Springer-Verlag, Berlin 1982.
[25] M.I. Dyakonov and V. Yu. Kachorovskii, Fiz. Tekh. Poluprovodn. **20**, 178 (1986) [Soviet Phys. – Semicond. **20**, 110 (1986)].
[26] J.M. Kikkawa and D.D. Awschalom, Science **287**, 473 (2000).